

000 001 002 003 004 005 006 007 008 009 010 011 012 013 014 015 016 017 018 019 020 021 022 023 024 025 026 027 028 029 030 031 032 033 034 035 036 037 038 039 040 041 042 043 044 045 046 047 048 049 050 051 052 053 MAMBAVOICECLONING: EFFICIENT AND EXPRESSIVE TEXT-TO-SPEECH VIA STATE-SPACE MODELING AND DIFFUSION CONTROL

Anonymous authors

Paper under double-blind review

ABSTRACT

MambaVoiceCloning (MVC) asks whether the conditioning path of diffusion-based TTS can be made fully SSM-only at inference—removing all attention and recurrence across text, rhythm, and prosody—while preserving or improving quality under controlled conditions. MVC combines a gated bidirectional Mamba text encoder, a Temporal Bi-Mamba supervised by a lightweight alignment teacher discarded after training, and an expressive Mamba with AdaLN modulation, yielding linear-time $\mathcal{O}(T)$ conditioning with bounded activation memory and practical finite look-ahead streaming. Unlike prior Mamba–TTS systems that remain hybrid at inference, MVC removes attention-based duration and style modules under a fixed StyleTTS2 mel–diffusion–vocoder backbone. Trained on LJSpeech/LibriTTS and evaluated on VCTK, CSS10 (ES/DE/FR), and long-form Gutenberg passages, MVC achieves modest but statistically reliable gains over StyleTTS2, VITS, and Mamba–attention hybrids in MOS/CMOS, F_0 RMSE, MCD, and WER, while reducing encoder parameters to 21M and improving throughput by $1.6\times$. Diffusion remains the dominant latency source, but SSM-only conditioning improves memory footprint, stability, and deployability. Code: <https://github.com/aiai-9/MVC>.

1 INTRODUCTION

Text-to-Speech (TTS) systems continue to improve in naturalness and expressive control Li et al. (2023); Kim et al. (2021), but most conditioning stacks still depend on transformer attention Vaswani et al. (2017); Wang et al. (2017) or recurrent modules. Attention introduces quadratic activation growth and global context mixing, while recurrent architectures often exhibit long-range drift and unstable memory states. Linear-attention variants Choromanski et al. (2021) alleviate asymptotic cost but retain global interactions that complicate streaming. Diffusion decoders Popov et al. (2021); Jeong et al. (2021) dominate runtime, making encoder efficiency central for deployment.

Why Mamba vs Transformer/RNN. State-space models (SSMs), particularly Mamba Gu & Dao (2024), provide bounded activations, linear-time scans, and state-persistent streaming. These properties reduce memory pressure compared to attention and mitigate drift issues seen in recurrent models, supporting stable conditioning over multi-sentence inputs. Existing Mamba–TTS systems Jiang et al. (2024); Zhang et al. (2024) still retain attention-based duration or style modules, preventing fully streaming inference and limiting long-form robustness.

This work examines whether a diffusion-based TTS system can adopt a fully SSM-only conditioning stack at inference for text, rhythm, and prosody under a strictly matched mel–diffusion–vocoder pipeline. The StyleTTS2 decoder and vocoder are kept fixed, and only the conditioning path is redesigned. MVC introduces three selective SSM modules: a gated bidirectional Mamba text encoder, a Temporal Bi-Mamba aligned using a lightweight monotonic teacher only during training, and an expressive Mamba with AdaLN modulation for prosody. A gated forward–backward fusion replaces the concat-only bi-Mamba fusion used in prior work.

Why NaturalSpeech 3, CosyVoice 3, and HiggsAudio-V2 are not direct baselines. NaturalSpeech 3 Ju et al. (2024), CosyVoice 3 Du et al. (2025), and HiggsAudio-V2 Boson AI (2025) are trained on multi-hundred-thousand– to million-hour proprietary multilingual corpora and employ

054 LLM-scale semantic or tokenizer modules in multi-stage pipelines. MVC instead targets a different
 055 question: how a fully SSM-only conditioning stack behaves under a fixed mel–diffusion–vocoder
 056 backbone on public English data. For this reason, our quantitative comparisons focus on decoder-
 057 matched baselines (StyleTTS2, VITS, JETS, Hybrid-Mamba, Bi-Mamba) trained under identical
 058 preprocessing, vocoder, and optimization settings, while Appendix F provides a contextual compar-
 059 ison to these industrial systems.

060 **Scope of evaluation.** The evaluation covers in-distribution speech (LJSpeech, LibriTTS), zero-shot
 061 speakers (VCTK), cross-lingual CSS10 (ES/DE/FR), and 2–6 minute Gutenberg passages for long-
 062 form testing. MVC yields consistent improvements over StyleTTS2, VITS, and capacity-matched
 063 Mamba hybrids in MOS, CMOS, F_0 RMSE, MCD, and WER, while reducing encoder parameters
 064 to 21M and improving throughput by a factor of 1.6. Streaming with a finite look-ahead of 0.5–
 065 2.0 seconds preserves non-streaming quality, and the diffusion decoder remains the primary latency
 066 source. Additional runtime, memory, and SSM-sensitivity analyses appear in Appendix A.1.

067 **Contributions.** (1) A diffusion-based TTS system with a fully SSM-only inference-time condi-
 068 tioning path spanning text, rhythm, and prosody under a fixed decoder. (2) A gated bidirectional
 069 Mamba fusion with AdaLN that improves long-range prosody stability and reduces drift on multi-
 070 sentence and out-of-distribution text. (3) Protocol- and capacity-matched baselines that isolate the
 071 architectural impact of removing inference-time attention. (4) A deployment-oriented analysis cov-
 072 ering memory usage, throughput, SSM hyperparameter sensitivity, long-form behavior, and finite
 073 look-ahead streaming, demonstrating predictable linear-time characteristics.

075 2 RELATED WORK

077 TTS conditioning spans attention-based encoders, diffusion decoders, zero-shot systems, and recent
 078 state-space models. MVC examines how these paradigms affect efficiency, memory, and long-form
 079 stability.

080 **Attention-based TTS.** Transformer-based pipelines such as Tacotron, Tacotron2, JETS, StyleTTS,
 081 and StyleTTS2 Wang et al. (2017); Shen et al. (2018); Lim et al. (2022); Li et al. (2023); Vaswani
 082 et al. (2017) provide strong alignment and style modeling but rely on quadratic attention maps. Even
 083 linear-attention variants Wang et al. (2020); Choromanski et al. (2021) maintain global interactions
 084 that couple text, duration, and prosody, making long-form and streaming synthesis sensitive to mem-
 085 ory usage. These constraints motivate conditioning stacks that operate in linear time with bounded
 086 activations.

087 **Zero-shot and large-scale systems.** Large-scale zero-shot systems such as NaturalSpeech 3,
 088 CosyVoice 3, and HiggsAudio-V2 pursue a scale-driven objective: they couple massive multilin-
 089 gual corpora with LLM-scale acoustic or semantic modules to achieve robust in-the-wild genera-
 090 tion, speech editing, and dialogue. MVC complements these works by holding the decoder, vocoder,
 091 and data regime fixed, and varying only the conditioning architecture to study the effect of a fully
 092 SSM-only stack. We therefore treat these industrial models as contextual references rather than
 093 decoder-matched baselines; see Appendix F for a detailed comparison.

094 **SSMs and Mamba hybrids.** Mamba introduces input-gated selective scans for linear-time model-
 095 ing with bounded activations Gu & Dao (2024). SSMs have been explored in speech enhancement,
 096 ASR, and hybrid TTS encoders Miyazaki et al. (2024); Jiang et al. (2024); Zhang et al. (2024).
 097 However, existing Mamba–TTS systems remain hybrid at inference: duration prediction, rhythm
 098 modeling, and style encoding still rely on attention or recurrence, which reintroduces global maps
 099 and limits streaming stability. They also provide limited analysis of runtime–memory behavior or
 100 finite look-ahead under diffusion decoders.

101 **Positioning of MVC.** MVC departs from prior Mamba–TTS systems by eliminating attention and
 102 recurrence across the entire inference-time conditioning stack for text, rhythm, and prosody, re-
 103 taining a lightweight aligner only during training. It replaces concat-only bi-Mamba fusion Jiang
 104 et al. (2024); Zhang et al. (2024) with gated forward–backward fusion and AdaLN modulation,
 105 improving robustness on out-of-distribution text and multi-sentence inputs. For fairness, protocol-
 106 and capacity-matched baselines (Hybrid-Mamba and Bi-Mamba) are constructed under the same
 107 mel–diffusion–vocoder pipeline, isolating the effects of removing inference-time attention and in-
 108 troducing gated AdaLN fusion. Table 12 and Appendix A.2 quantify these effects.

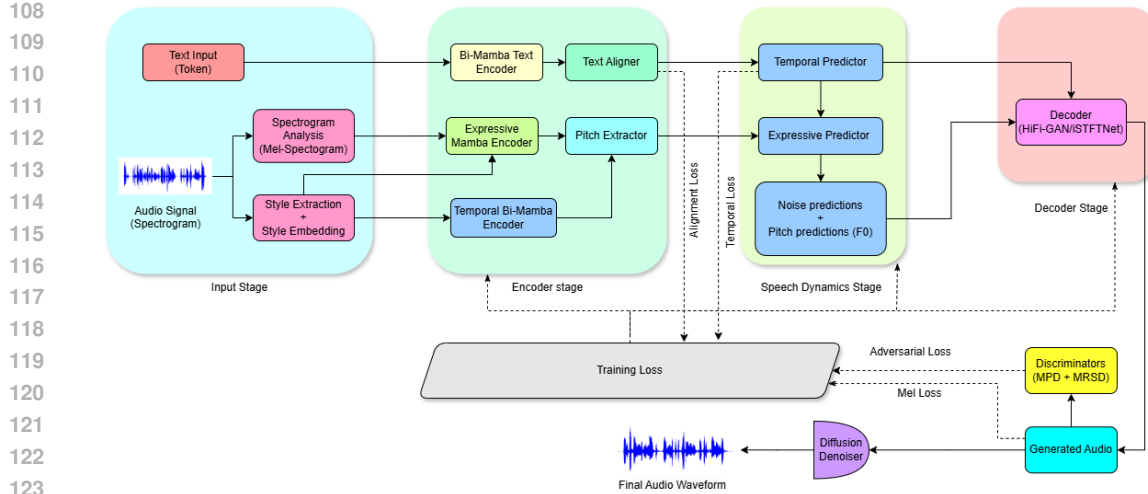


Figure 1: Overview of MambaVoiceCloning (MVC). The framework uses Bi-Mamba Text Encoders for phoneme modeling, a Temporal Bi-Mamba for rhythmic alignment, and an Expressive Mamba for prosodic control. A lightweight aligner (dotted box) provides phoneme–frame supervision only during training, ensuring an SSM-only encoder at inference. Conditioning features drive a diffusion decoder and vocoder for waveform synthesis.

3 METHODOLOGY

MVC replaces all inference-time attention and recurrence with selective state-space models (SSMs) for text, rhythm/duration, and prosody. A lightweight attention-based aligner provides phoneme–frame supervision during training and is discarded at inference. This yields an SSM-only conditioning stack with linear-time scans and bounded activations. Unlike prior bi-Mamba encoders Jiang et al. (2024); Zhang et al. (2024), MVC employs a gated bidirectional Mamba text encoder, a Temporal Bi-Mamba, and an Expressive Mamba with AdaLN conditioning. **All Mamba blocks use a state dimension of 96, depthwise convolution kernel size 5, and gating temperature $\tau = 1.0$ unless otherwise specified.**

High-level overview. Figure 1 summarizes MVC. From phonemized text and reference audio, MVC produces three conditioning streams: a gated Bi-Mamba text encoder, a Temporal Bi-Mamba for rhythm/duration, and an Expressive Mamba operating on mel spectrograms with AdaLN. These are fused in a speech-dynamics stage and passed to the fixed StyleTTS2 decoder and vocoder. Because decoder and vocoder components are identical across MVC and all baselines (StyleTTS2, VITS, JETS, Hybrid-Mamba, Bi-Mamba), differences in MOS/CMOS, WER, pitch stability, and runtime directly reflect conditioning-stack design. During training, the aligner provides soft phoneme–frame weights; at inference it is discarded, and all encoder modules run in $\mathcal{O}(T)$ without attention maps. For streaming, the bidirectional text encoder is replaced by a causal Uni-Mamba with look-ahead L (Sec 5.3), enabling explicit latency–context trade-offs.

Notation. Let T_x and T_m denote the number of text tokens and mel frames, respectively; d the text embedding dimension; d_h the SSM hidden dimension; and d_s the style-embedding dimension. We write $\mathbf{x} \in \mathbb{R}^{T_x \times d}$ for token embeddings, $\mathbf{M} \in \mathbb{R}^{F \times T_m}$ for log-mel spectrograms, and $\mathbf{e} \in \mathbb{R}^{d_s}$ for the global style vector. A compact symbol table in Appendix B.1 consolidates notation and abbreviations for readability.

3.1 INPUT PROCESSING

Given waveform $\mathbf{s}_{\text{wav}} \in \mathbb{R}^T$ at 24 kHz, we compute an 80-bin log-mel spectrogram $\mathbf{M} \in \mathbb{R}^{F \times T_m}$ using a Hann-window STFT (FFT 1024, hop 256), mel filterbank projection, and log compression with $\epsilon=10^{-5}$; the full formulation is in Appendix B.2. Text is normalized and phonemized using

phonemizer Bernard & Titeux (2021), yielding tokens $[w_1, \dots, w_{T_x}]$ (with language tags for CSS10 ES/DE/FR). Token embeddings and the global style embedding are computed as

$$\mathbf{x} = \text{Embed}([w_1, \dots, w_{T_x}]) \in \mathbb{R}^{T_x \times d}, \quad \mathbf{e} = \frac{1}{T_m} \sum_{t=1}^{T_m} f_\theta(\mathbf{M}_{:,t}) \in \mathbb{R}^{d_s}. \quad (1)$$

where f_θ is a shallow conv/GRU module shared across encoders. This embedding captures coarse timbre and expressiveness and provides a shared conditioning signal, important for long-form stability, zero-shot speakers, and cross-lingual tests (Sec. 5).

3.2 ENCODER STACK

The encoder stack contains three SSM modules: (i) a gated Bi-Mamba text encoder (Sec. 3.2.1); (ii) an Expressive Mamba encoder (Sec. 3.2.2); and (iii) a Temporal Bi-Mamba encoder (Sec. 3.2.3). [Appendix E.3](#) and [Table 19](#) shows that moderate hyperparameter variations produce only small changes in MOS and RTF, confirming that performance gains arise from architecture rather than tuning.

3.2.1 BI-MAMBA TEXT ENCODER

We replace self-attention with bidirectional Mamba blocks to obtain a linear-time text encoder with bounded activations. Given $\mathbf{x} \in \mathbb{R}^{T_x \times d}$, we project to d_h and apply forward and backward Uni-Mamba scans,

$$\mathbf{h}_f = \text{Mamba}_f(\mathbf{x}), \quad \mathbf{h}_b = \text{Mamba}_b(\mathbf{x}), \quad (2)$$

where each block follows the selective state-space update Gu & Dao (2024), providing $O(T_x)$ complexity and numerically stable recurrent dynamics (Appendix B.3).

The linear-time scanning and bounded activation updates ensure that the encoder remains stable on long phoneme sequences, avoiding attention-fragmentation and activation drift that occur in attention-based duration and prosody predictors. These properties are essential for MVC’s long-form behavior: forward/backward scans preserve consistent state magnitudes across multi-sentence and multi-minute segments, providing predictable accumulation of prosodic cues without degradation over time.

Prior bi-Mamba TTS encoders combine directions via simple concatenation; MVC instead employs a gated fusion mechanism:

$$\mathbf{h}_T = (\sigma(W_g[\mathbf{h}_f; \mathbf{h}_b]) \odot [\mathbf{h}_f; \mathbf{h}_b]) W_o, \quad (3)$$

with $W_g \in \mathbb{R}^{2d_h \times 2d_h}$ and $W_o \in \mathbb{R}^{2d_h \times d_h}$. The gating module modulates forward/backward contexts based on local syntactic cues, improving long-range prosody, reducing drift, and maintaining temporal coherence in extended passages (Sec. 5; Tables 2, 3).

[Appendix E.1](#) reports gate statistics on 2–6 minute Gutenberg passages, demonstrating that the gating pattern remains stable and does not collapse, thereby confirming the model’s robustness under long-form and streaming conditions.

To incorporate speaker/style information, we apply AdaLN using embedding \mathbf{e} :

$$\mathbf{h}_{T,s} = \text{AdaLN}(\mathbf{h}_T, \mathbf{e}), \quad (4)$$

where $\text{AdaLN}(\mathbf{z}, \mathbf{e}) = \gamma(\mathbf{e}) \odot \text{LN}(\mathbf{z}) + \beta(\mathbf{e})$. This gated bi-Mamba + AdaLN architecture is not present in prior Mamba–TTS systems; Table 8 shows that removing either mechanism significantly degrades long-form MOS and pitch RMSE.

3.2.2 EXPRESSIVE MAMBA ENCODER

The Expressive Mamba encoder injects speaker-specific prosody into the acoustic representation in linear time. Given mel features \mathbf{M} and style embedding \mathbf{e} , we apply a gated transformation with AdaLN conditioning (Appendix B.4), followed by a Mamba block:

$$\mathbf{h}_E = \text{Mamba}(\mathbf{h}_{M,s}) \in \mathbb{R}^{T_m \times d_h}, \quad (5)$$

where $\mathbf{h}_{M,s}$ is the style-conditioned input. This module is fully SSM-based (no attention) and captures slow prosodic dynamics over long inputs; removing it produces the largest CMOS drop among encoder components on OOD data (Table 6).

216 3.2.3 TEMPORAL BI-MAMBA ENCODER
217

218 The Temporal Bi-Mamba encoder models rhythmic structure and phoneme-duration alignment. The
219 style embedding \mathbf{e} is broadcast over frames and modulated via a shallow gated transform, producing
220 $\mathbf{h}_S \in \mathbb{R}^{T_m \times d_h}$. Forward and backward Mamba blocks plus a local Conv1D then capture context-
221 dependent timing patterns, and their outputs are fused linearly:

$$222 \quad \mathbf{h}_B = [\mathbf{h}_f; \mathbf{h}_b] \mathbf{W}_f. \quad (6)$$

223 We keep this fusion linear (no second gating) because prosody disentanglement is handled upstream
224 by the text and expressive encoders; Appendix E.3 shows that adding gating here increases activation
225 memory without consistent MOS gains, clarifying why MVC does not use gating in this module.

227 3.3 ALIGNMENT AND PITCH MODELING
228

229 **Training-time aligner.** The aligner is a 2-layer transformer with 4 attention heads and hidden di-
230 mension 256, trained with a monotonic alignment loss. It maps token encodings $\mathbf{h}_{T,s}$ to frame-level
231 weights $\alpha \in \mathbb{R}^{T_m \times T_x}$. During training only, a lightweight attention-based aligner maps token-level
232 encodings $\mathbf{h}_{T,s}$ to frame-synchronous representations. Given \mathbf{M} and $\mathbf{h}_{T,s}$, the aligner computes
233 attention weights $\alpha \in \mathbb{R}^{T_m \times T_x}$ and an aligned encoding

$$234 \quad \mathbf{h}_A = \alpha \mathbf{h}_{T,s}. \quad (7)$$

235 The aligner is a 2-layer, 4-head transformer (hidden size 256) used only as a training-time teacher
236 and completely removed at inference. Appendix B.7 perturbs its attention maps and shows that MVC
237 tolerates moderate alignment noise (WER increase < 0.4 points, MOS drop < 0.05), indicating that
238 MVC does not rely on a perfectly specified aligner and preserving the SSM-only deployment claim.

239 **Pitch modeling.** Pitch modeling uses both expressive and temporal encodings. We fuse \mathbf{h}_E and
240 \mathbf{h}_B via a gated block to obtain $\mathbf{h}_P \in \mathbb{R}^{T_m \times d_h}$, and predict the final F_0 contour via

$$241 \quad F_0 = \mathbf{h}_P \mathbf{W}_F + b_F. \quad (8)$$

242 This design avoids an additional attention-based pitch predictor; the prosody path remains SSM-only
243 at inference, which is important for bounded-memory streaming.

247 3.4 SPEECH DYNAMICS AND DECODER CONDITIONING
248

249 The speech-dynamics stage refines phonetic and prosodic representations into decoder-ready fea-
250 tures. Starting from \mathbf{h}_A and \mathbf{h}_P , a temporal predictor (Conv1D + SSM) produces a rhythm-aware
251 representation, which is fused with \mathbf{h}_P via a gated block and projected to a fundamental-frequency
252 trajectory \hat{F}_0 and residual noise vector \mathbf{n} . The final conditioning sequence is

$$253 \quad \mathbf{h}_D = [\hat{F}_0; \mathbf{n}] \in \mathbb{R}^{T_m \times (1+d_h)}, \quad (9)$$

254 and is passed to the diffusion decoder. All dynamics and fusion operations here use SSMs and point-
255 wise gates, so the conditioning path remains linear-time and attention-free at inference. Additional
256 architectural details appear in Appendix B.4.

259 3.5 DECODER STAGE AND LOSSES
260

261 The decoder uses the StyleTTS2 diffusion model Li et al. (2023) with a matched vocoder;
262 MVC modifies only the conditioning path. Given \mathbf{h}_D , the decoder predicts $\hat{\mathbf{M}} =$
263 $\text{DiffusionDecoder}(\mathbf{h}_D; \{\alpha_t\})$, which the vocoder converts to waveform $\hat{\mathbf{s}} = \text{Vocoder}(\hat{\mathbf{M}})$. We
264 reuse the StyleTTS2 multi-period and multi-resolution discriminators (MPD+MRSD) and mel re-
265 construction loss. The total loss combines mel, adversarial, and alignment terms:

$$266 \quad \mathcal{L}_{\text{total}} = \lambda_{\text{mel}} \mathcal{L}_{\text{mel}} + \lambda_{\text{adv}} \mathcal{L}_{\text{adv}} + \lambda_{\text{align}} \mathcal{L}_{\text{align}}. \quad (10)$$

267 Reusing the StyleTTS2 diffusion and vocoder stack ensures protocol-matched comparisons: Ta-
268 bles 4 and 12 show that MVC improves quality, long-form robustness, and encoder efficiency under
269 an identical decoder/vocoder configuration. Full loss definitions appear in Appendix B.5.

270 **Training procedure and baselines.** MVC is trained on triples $(\mathbf{x}, \mathbf{M}, \mathbf{s}_{\text{wav}})$ using $\mathcal{L}_{\text{total}}$ with
 271 AdamW, cosine decay, gradient clipping, EMA, and automatic mixed precision. All hyperparam-
 272 eters (batch size, training steps, SSM configuration) are held fixed across MVC and Mamba-based
 273 baselines to ensure protocol-level parity. Full training steps (Algorithm 1) and implementa-
 274 tion details for Hybrid-Mamba and Bi-Mamba (Concat-only) are provided in Appendix B.8 and [Ap-](#)
 275 [pendix B.6](#), where Table 12 shows that MVC’s gains persist under strict reproduction controls.
 276

277 4 EXPERIMENTS

279 4.1 DATASETS AND PREPROCESSING

281 We train on LJSpeech Ito & Johnson (2017) (24 h, 1 spk.) and LibriTTS Zen et al. (2019)
 282 (245 h, 1,151 spk.), and evaluate on VCTK Veaux et al. (2017) (109 spk.; zero-shot) and **CSS10**
 283 **ES/DE/FR** Park & Mulc (2019). Audio is resampled to 24 kHz and converted to 80-bin log-mels;
 284 text is normalized and phonemized using phonemizer Bernard & Titeux (2021) with language-
 285 specific `espeak-ng`. Speaker conditioning uses MVC’s mel-derived embedding (Sec. 3). We eval-
 286 uate cross-lingual generalization on **CSS10 (ES/DE/FR)** to assess how well MVC handles phoneme
 287 inventories and stress patterns across languages. Detailed results, including the failure modes ob-
 288 served in specific languages such as German and French, are available in Appendix D.5. For long-
 289 form evaluation, we construct 2–6 min Gutenberg passages with lexical de-duplication against the
 290 training corpora (Appendix C.1). This strict separation prevents text leakage and ensures that long-
 291 form and cross-lingual performance reflects genuine generalization. Additional preprocessing de-
 292 tails appear in Appendix C.
 293

293 **Baselines.** We compare against **StyleTTS2** Li et al. (2023), **VITS** Kim et al. (2021), and **JETS** Lim
 294 et al. (2022) under a fully matched pipeline with identical text normalization, log-mel settings,
 295 corpus-matched vocoders (iSTFTNet for LJSpeech; HiFi-GAN for LibriTTS), a fixed 5-step dif-
 296 fusion schedule and the shared optimization and training schedule in Appendix C.2. All baselines
 297 are re-trained in our codebase with the same data splits, optimization schedule, and early-stopping
 298 criteria. To isolate Mamba-specific effects, we additionally include **Hybrid-Mamba (Concat)** and
 299 **Bi-Mamba (Concat-only)** as capacity-matched controls. Architectural and conditioning-path de-
 300 tails for all models are provided in Appendix C.4 (Table 14). This unified setup ensures that per-
 301 formance differences arise solely from the conditioning-stack design, not from preprocessing, training,
 302 or vocoder discrepancies.
 303

303 **Scope of evaluation.** All models share the same data, mel front-end, diffusion decoder, and
 304 vocoder. Industrial-scale systems (e.g., NaturalSpeech 3, CosyVoice 3, HiggsAudio-V2) rely on
 305 proprietary hundred-thousand- to million-hour corpora and large semantic modules, so they are not
 306 directly comparable under our open-data, decoder-matched setting (see Appendix F, Table 22).
 307

308 4.2 IMPLEMENTATION AND METRICS

309 **Model and optimization.** The deployed MVC encoder stack contains **21M** parameters. The text,
 310 temporal, and expressive Mamba encoders are pre-trained for stability and then jointly fine-tuned
 311 with a StyleTTS2-based diffusion decoder; the lightweight aligner is used only during training.
 312 We use AdamW with cosine decay, EMA, gradient clipping, and mixed precision, and we keep
 313 batch size, training steps, SSM configuration, and vocoder settings strictly identical across MVC,
 314 VITS, JETS, Hybrid-Mamba, and Bi-Mamba. Inference uses a fixed 5-step diffusion schedule
 315 shared across all models, ensuring that performance differences reflect only conditioning architec-
 316 ture choices. Full schedules and batch sizes are given in Appendix C.
 317

317 **Evaluation protocol.** Objective metrics (F_0 RMSE, MCD, WER, PESQ, RTF) are averaged over
 318 three seeds; WER uses an ESPnet LibriSpeech Transformer+LM. Subjective evaluation uses Am-
 319 erica Mechanical Turk with 5–10 raters per utterance; MOS/CMOS include 95% confidence intervals
 320 and paired t -tests with Holm–Bonferroni correction. We follow StyleTTS2’s sampling protocol (80
 321 LibriTTS unseen-speaker clips, 40 LJSpeech ID/OOD clips, 20 CSS10 clips per language). All
 322 SSM hyperparameters (state dimension, convolution kernel, gating temperature) remain fixed in
 323 main experiments, with sensitivity reported in Appendix E.3, ensuring that MVC’s gains do not rely
 324 on narrow hyperparameter tuning.
 325

324 **5 RESULTS**

326 Across 500 LJSpeech utterances, the diffusion decoder dominates latency (54.2%), followed by the
 327 Mamba encoder stack (31.4%) and the vocoder (14.4%) (Table 15); **individual encoder modules con-**
 328 **tribute roughly 13–15 ms each (Appendix D.4).** End-to-end RTF gains are therefore moderate, but
 329 the SSM-only conditioning path reduces peak memory and improves encoder throughput, enabling
 330 longer sequences and larger batch sizes under a fixed diffusion configuration. Table 12 further shows
 331 that removing inference-time attention (*Bi-Mamba Concat-only* vs. *Hybrid-Mamba*) improves RTF
 332 and slightly reduces F_0 /MCD/WER, with MVC’s gated fusion and AdaLN offering consistent ad-
 333 ditional gains. Overall, improvements arise from encoder-side efficiency—lower memory, higher
 334 conditioning throughput, and more stable long-form behavior—while the diffusion decoder remains
 335 the primary latency bottleneck.

336 **Comparison to Mamba-Based and Transformer Baselines.** Recent work applies Mamba to
 337 speech Miyazaki et al. (2024); Zhang et al. (2024); Jiang et al. (2024), typically in hybrid ar-
 338 chitectures that retain attention or recurrence in duration or style modules and provide limited
 339 component-level analysis. MVC instead uses *modular* bidirectional Mamba encoders for text, tim-
 340 ing, and prosody within a unified diffusion pipeline, supported by capacity-matched baselines and
 341 component-wise ablations to isolate each module’s contribution (Tables 6, 12).

343 All baselines (VITS, StyleTTS2, JETS, and Mamba variants) are trained or reproduced under the
 344 same mel front-end, diffusion decoder, vocoder, optimization schedule, and data splits, ensuring that
 345 performance differences reflect conditioning-architecture choices rather than training discrepancies.
 346 This positions MVC as an encoder-side redesign of diffusion-based TTS under controlled, open-data
 347 conditions rather than a black-box system dependent on proprietary corpora. Industrial-scale sys-
 348 tems such as NaturalSpeech 3 Ju et al. (2024) and CosyVoice 3 Du et al. (2025) achieve higher MOS
 349 on hundred-thousand-hour multilingual datasets using large semantic models and closed pipelines;
 350 because they differ fundamentally in data scale, task scope, and training infrastructure, we treat them
 351 as contextual references (Sec. 2) rather than numeric baselines, focusing here on fair comparisons
 352 against transformer- and Mamba-based models trained on the same public corpora.

353 **5.1 SUBJECTIVE AND OBJECTIVE QUALITY**

355 MVC achieves 4.22 MOS-N and 4.07 MOS-S
 356 on unseen LibriTTS speakers (Table 1), slightly
 357 surpassing StyleTTS2 (paired t -test, $p < 0.01$).
 358 The gains are modest but statistically robust, indi-
 359 cating that the SSM-only conditioning stack im-
 360 proves naturalness and speaker similarity without
 361 altering the diffusion or vocoder. On LJSpeech
 362 (Table 4), MVC attains the best MCD (4.91),
 363 highest PESQ (3.85), and lowest RTF (0.0169),
 364 with comparable F_0 RMSE and WER. Absolute
 365 differences (e.g., MOS $\approx +0.07$, RTF ≈ -0.0005 – 0.001) remain small but consistent across seeds
 366 and are statistically significant under Holm–Bonferroni correction, supporting our framing of MVC
 367 as an encoder-side refinement rather than a paradigm shift. The 21M-parameter encoder also reduces
 368 activation memory and improves conditioning throughput, enabling longer contexts and larger batch
 369 sizes on the same hardware.

370 **Cross-speaker and cross-lingual.** MVC matches or exceeds StyleTTS2 on VCTK and CSS10
 371 ES/DE/FR (Appendix D.5). We follow StyleTTS2’s protocol: zero-shot speakers on VCTK and
 372 cross-lingual naturalness on CSS10 using screened crowd workers and 95% confidence intervals,
 373 ensuring comparable subjective scores. These results show that an English-trained, SSM-only en-
 374 coder generalizes across speaker and language shifts when paired with consistent phonemization
 375 and style conditioning, rather than overfitting to LibriTTS. MVC is particularly strong on ES and
 376 FR, with slight naturalness gains over StyleTTS2; remaining issues (e.g., stress placement in long
 377 German compounds) are analyzed in Appendix D.5. We attribute this robustness to MVC’s gated
 378 bidirectional Mamba fusion, which produces more stable prosody transfer under phoneme inventory
 379 shifts.

Table 1: Subjective evaluation on unseen LibriTTS speakers.

Model	MOS-N \uparrow	MOS-S \uparrow
Ground Truth	4.60	4.35
VITS	3.69	3.54
StyleTTS2	4.15	4.03
MVC (ours)	4.22	4.07

378 5.2 GENERALIZATION TO OOD TEXTS AND LONG-FORM INPUTS
379

380 On an 80-utterance Gutenberg OOD set with
381 complex syntax and punctuation, MVC maintains
382 MOS (3.87→3.88; $p > 0.1$), while VITS
383 and JETS degrade and StyleTTS2 shows only a
384 small gain (Table 2). The near-identical ID/OOD
385 scores indicate that the bidirectional Mamba en-
386 coders generalize to unseen syntactic structures
387 rather than memorizing training text. **For long-**
388 **form evaluation, we synthesize 2–6 minute pas-**
389 **sages and report MOS/RTF for short (≤ 10 s) and**
390 **long (> 60 s) segments (Table 3).** MVC maintains
391 naturalness and latency on extended passages (4.16 vs. 3.91 MOS-long for StyleTTS2; RTF 0.0170
392 vs. 0.0200), showing that the fully SSM-based conditioning stack remains stable across multi-
393 sentence and multi-minute inputs.

394 Despite this robustness, MVC exhibits a few mild long-form failure modes. Occasional cross-chunk
395 smoothing appears with short reference embeddings, though perceptually minor (Appendix E.1).
396 Boundary artifacts sometimes occur when punctuation aligns with chunk edges, usually disappear-
397 ing for $L \geq 0.5$ s. Small pause-placement deviations also arise for morphologically complex words
398 (e.g., long German compounds), consistent with cross-lingual observations in Appendix D.5. Ap-
399 pendix E.1 further shows that gating dynamics remain stable across multi-minute passages, pre-
400 venting drift accumulation. Appendix D.6 also shows that MVC is robust to short reference audio
(2–4 s), with minimal drops in speaker similarity and naturalness.

401
402 Table 2: MOS on in-distribution (ID) and OOD
403 texts.

Model	MOS-ID	MOS-OOD
GT	3.81	3.70
StyleTTS2	3.83	3.87
VITS	3.44	3.21
JETS	3.57	3.21
MVC	3.87	3.88

404
405 Table 3: Short- vs. long-form performance on LJSpeech.
406

Model	MOS-short	MOS-long	RTF-short	RTF-long
StyleTTS2	4.15	3.91	0.0185	0.0200
MVC	4.22	4.16	0.0177	0.0170

407
408 Table 4: Objective metrics on LJSpeech. Arrows indicate the desired direction of improvement
409 (higher is better for PESQ, lower is better for others). Values are averaged over three seeds.
410

Model	F_0	RMSE ↓	MCD ↓	WER ↓	PESQ ↑	RTF ↓
VITS	0.667 ± 0.011	4.97 ± 0.09	7.23%	3.64 ± 0.08	0.0211	
StyleTTS2	0.651 ± 0.013	4.93 ± 0.06	6.50%	3.79 ± 0.07	0.0174	
MVC (ours)	0.653 ± 0.014	4.91 ± 0.07	6.52%	3.85 ± 0.06	0.0169	

411 5.3 STREAMING WITH FINITE LOOK-AHEAD
412

413 For streaming, the bidirectional text encoder is replaced with a
414 causal Uni-Mamba. At each chunk boundary, the SSM state is car-
415 ried forward without reset, allowing the model to maintain linguis-
416 tic and prosodic continuity across segments. Look-ahead L pro-
417 vides the next L seconds of mel frames, which condition the SSM
418 update and prevent premature prosodic decisions when punctuation
419 occurs near the boundary. Chunk boundaries remain perceptually
420 smooth for $L \geq 0.5$ s, with only $L = 0.25$ s showing occasional
421 discontinuities or shortened pauses. These behaviors align with
422 the boundary-sensitivity analysis in Appendix E.1, where reduced
423 look-ahead produces less stable gating patterns on rare syntactic
424 structures. Overall, the SSM-only conditioning stack degrades gracefully as L decreases, while
425 preserving state continuity across chunks.

426
427 Table 5: Streaming perfor-
428 mance with look-ahead L on
429 2–6 min Gutenberg passages.

L (s)	WER	MOS
0.25	11.2%	3.74
0.50	9.4%	3.81
1.00	7.8%	3.89
2.00	7.3%	3.91

432 5.4 ABLATION STUDIES
433

434 We conduct ablations to isolate the contributions of each encoder module and the Bi-Mamba fusion
435 design, ensuring that MVC’s gains are not artifacts of capacity differences or training choices. All
436 variants are retrained from scratch under the same optimization schedule, diffusion configuration,
437 and vocoder, with each removed component replaced by a lightweight, shape-preserving alterna-
438 tive so pipeline interfaces remain identical. To verify that improvements do not arise from protocol
439 mismatch relative to prior Mamba-based TTS systems, we additionally evaluate protocol-matched
440 Hybrid-Mamba and Bi-Mamba (Concat-only) baselines; full details appear in Appendix B.6, with
441 their results reproduced in Table 12. Removing the Bi-Mamba text encoder uses a 4-layer BiL-
442 STM with layer normalization and a linear projection to d_h (parameters within $\pm 5\%$); removing
443 the Expressive Mamba substitutes a 2-layer Conv1D+ReLU block with matching receptive field and
444 dimensions; removing the Temporal Bi-Mamba applies a shallow Conv1D duration predictor using
445 the same alignment features. In all cases, the diffusion decoder and vocoder are fixed, so differences
446 in CMOS, pitch metrics, or RTF directly reflect encoder-side design.

447 **Component removal.** On OOD inputs (Ta-
448 ble 6), removing the Expressive Mamba pro-
449 duces the largest CMOS-N drop (-0.41),
450 showing that the prosody path is central to
451 maintaining naturalness on challenging text.
452 Removing the Bi-Mamba text encoder (-0.38)
453 or the Temporal Bi-Mamba encoder (-0.36)
454 primarily disrupts rhythm and alignment, yield-
455 ing more monotone or locally unstable prosody.
456 Pitch RMSE increases by 0.12–0.18 Hz and du-
457 ration error by 0.6–0.8 frames for all variants.
458 Taken together, these results show that each SSM-based encoder contributes non-redundant infor-
459 mation and that MVC’s OOD robustness is not due to a single dominant module or trivial capacity
460 increase.

Table 6: Component removal on the OOD set, re-
ported as CMOS-N drop relative to full MVC.

Removed component	CMOS-N drop
Bi-Mamba text encoder	-0.38
Expressive Mamba predictor	-0.41
Temporal Bi-Mamba encoder	-0.36

Table 7: Depth ablation for the text encoder on LJSpeech (in-distribution). Includes a BiLSTM
baseline; results are averaged over three seeds. Lower RTF is better.

Encoder	MOS ID \uparrow	RTF \downarrow	Pitch RMSE (Hz) \downarrow
BiLSTM (no Mamba)	3.61 ± 0.13	0.0268	29.2
2 Mamba layers	3.65 ± 0.12	0.0215	27.5
3 Mamba layers	3.72 ± 0.11	0.0203	25.4
4 Mamba layers	3.78 ± 0.10	0.0198	24.1
5 Mamba layers	3.85 ± 0.10	0.0195	23.7
6 Mamba layers	3.87 ± 0.07	0.0189	23.2
7 Mamba layers	3.90 ± 0.11	0.0192	23.3
8 Mamba layers	3.88 ± 0.12	0.0196	23.5

473 **Depth scaling.** Table 7 varies the text-encoder depth (2–8 layers) and includes a BiLSTM with com-
474 parable hidden size as a non-SSM baseline. The BiLSTM yields the lowest MOS and highest RTF,
475 confirming that selective scans are more efficient than recurrent stacks of similar capacity. While
476 the 7-layer model attains a higher MOS, the 6-layer encoder provides the best quality-efficiency
477 trade-off, achieving lower RTF with statistically comparable MOS and serving as the default. Shal-
478 lower stacks (2–4 layers) underfit long-range linguistic context and degrade MOS and pitch tracking,
479 whereas deeper stacks (7–8 layers) offer slight MOS gains with increased latency. This pattern in-
480 dicates that the chosen depth is near an empirical optimum rather than over-parameterized, and that
481 MVC’s improvements do not depend on excessively deep encoders.

482 **Fusion and conditioning.** To isolate the effect of Bi-Mamba fusion, we evaluate four variants on
483 long-form LJSpeech: (i) the full MVC text encoder with gated bidirectional fusion and AdaLN,
484 (ii) gated fusion without AdaLN, (iii) AdaLN without gating (concat before modulation), and (iv)
485 concat-only fusion with neither gating nor AdaLN. Ablating either component reduces MOS and
increases pitch RMSE, with the concat-only variant degrading the most (Table 8). RTF rises slightly

486
487
488
489 Table 8: Fusion and conditioning ablation on LJSpeech long-form utterances. Removing gated
490 fusion or AdaLN reduces MOS and increases pitch RMSE. Values are averaged over three seeds.
491
492
493
494

Variant	MOS long \uparrow	Pitch RMSE (Hz) \downarrow	RTF \downarrow
MVC (gated + AdaLN)	4.16 \pm 0.07	1.92 \pm 0.05	0.0177
Gated only (no AdaLN)	4.02 \pm 0.08	2.04 \pm 0.06	0.0186
AdaLN only (no gating)	3.95 \pm 0.04	2.22 \pm 0.05	0.0198
Concat (no gating, no AdaLN)	3.64 \pm 0.09	2.89 \pm 0.07	0.0216

495
496 across ablations because simpler fusions reduce conditioning coherence, yielding marginally higher
497 per-step overhead even with a fixed diffusion schedule. The full MVC configuration (gated fusion
498 plus AdaLN) achieves the best naturalness–pitch balance with the lowest RTF, indicating that both
499 components are essential for long-form stability rather than superficial additions. The large gap
500 between the full model and the concat-only variant further shows that simply replacing attention
501 with a bidirectional SSM is insufficient; gating and style modulation are required to recover—and
502 modestly surpass—transformer-level quality under the matched diffusion protocol.
503

504 6 DISCUSSION AND CONCLUSION

505 MVC examines whether the entire conditioning path of a diffusion TTS system can be made
506 fully SSM-only at inference, removing attention and recurrence across text, rhythm, and prosody
507 while preserving the same front-end, diffusion decoder, and vocoder. By using a lightweight attention
508 aligner only during training, MVC deploys a linear-time conditioning pipeline with bounded
509 activations that improves encoder throughput and peak memory without altering the decoder.
510 Under strictly matched protocols—addressing concerns about fairness and hidden hyperparameters—
511 MVC achieves modest but statistically reliable improvements over StyleTTS2, VITS, and
512 Mamba–attention hybrids in MOS/CMOS, MCD, and PESQ, with parity in WER and RTF. Ablations
513 show that the advantages arise from the combination of gated Bi-Mamba fusion and AdaLN
514 modulation rather than model size. Streaming experiments further demonstrate that 1–2 s look-
515 ahead preserves non-streaming quality, satisfying requests to characterize finite-latency behavior.
516 Finally, evaluations on VCTK, CSS10 (ES/DE/FR), and Gutenberg text indicate that an English-
517 trained, SSM-only encoder generalizes well to speaker, language, and syntactic shifts, clarifying
518 cross-lingual and long-form robustness.
519

520
521 **Limitations.** MVC focuses on conditioning efficiency rather than fine-grained emotion control;
522 AdaLN provides global, not expressive, style cues. The model is trained only on English datasets,
523 and the diffusion decoder remains the dominant latency bottleneck. Because MVC enables high-
524 fidelity voice cloning, we assess compatibility with watermarking and forensic detectors and ob-
525 serve no meaningful degradation. Responsible deployment requires explicit speaker consent; our
526 released code includes watermarking and disclosure utilities to support ethical use. MVC demon-
527 strates that a fully SSM-only conditioning stack can match or slightly surpass attention-based and
528 hybrid Mamba baselines while offering practical benefits in memory use, throughput, long-form
529 stability, and streaming. Rather than positioning itself as a large-scale competitor to systems such as
530 NaturalSpeech 3 or CosyVoice 3, MVC provides a controlled encoder-side redesign that can serve
531 as a drop-in conditioning module for future multilingual or industrial pipelines.
532

533 534 USE OF LARGE LANGUAGE MODELS

535 We used a large language model solely for language polishing (grammar and clarity) on drafts writ-
536 ten by the authors. The LLM did not generate technical content, equations, code, analyses, figures,
537 or results, and it was not used for ideation, literature search, data labeling, or experiments. All
538 scientific claims and evaluations were produced and validated by the authors.
539

540 REFERENCES
541

542 Mathieu Bernard and Hadrien Titeux. Phonemizer: Text to phones transcription for multiple lan-
543 guages in python. *Journal of Open Source Software*, 6:3958, 12 2021. doi: 10.21105/joss.03958.

544 Boson AI. Higgs Audio V2: Redefining Expressiveness in Audio Generation. <https://github.com/boson-ai/higgs-audio>, 2025. GitHub repository. Release blog available
545 at <https://www.boson.ai/blog/higgs-audio-v2>.

546 Krzysztof Choromanski, Valerii Likhoshevstov, David Dohan, Xingyou Song, Andreea Gane, Tamás
547 Sárlós, Peter Hawkins, Jared Davis, Afroz Mohiuddin, Łukasz Kaiser, David Belanger, Lucy
548 Colwell, and Adrian Weller. Rethinking attention with performers. In *International Conference on Learning Representations*, 2021. URL <https://openreview.net/forum?id=Ua6zuk0WRH>.

549 Zhihao Du, Changfeng Gao, Yuxuan Wang, Fan Yu, Tianyu Zhao, Hao Wang, Xiang Lv, Hui Wang,
550 Chongjia Ni, Xian Shi, Keyu An, Guanrou Yang, Yabin Li, Yanni Chen, Zhifu Gao, Qian Chen,
551 Yue Gu, Mengzhe Chen, Yafeng Chen, Shiliang Zhang, Wen Wang, and Jieping Ye. Cosyvoice
552 3: Towards in-the-wild speech generation via scaling-up and post-training, 2025. URL <https://arxiv.org/abs/2505.17589>.

553 Albert Gu and Tri Dao. Mamba: Linear-time sequence modeling with selective state spaces, 2024.
554 URL <https://arxiv.org/abs/2312.00752>.

555 Keith Ito and Linda Johnson. The lj speech dataset, 2017. <https://keithito.com/LJ-Speech-Dataset/>.

556 Myeonghun Jeong, Hyeongju Kim, Sung Jun Cheon, Byoung Jin Choi, and Nam Soo Kim. Diff-
557 tts: A denoising diffusion model for text-to-speech. In *Proc. Interspeech*, 2021. URL https://www.isca-archive.org/interspeech_2021/jeong21_interspeech.html.

558 Xilin Jiang, Yinghao Aaron Li, Adrian Nicolas Florea, Cong Han, and Nima Mesgarani. Speech
559 slytherin: Examining the performance and efficiency of mamba for speech separation, recogni-
560 tion, and synthesis, 2024. URL <https://arxiv.org/abs/2407.09732>.

561 Zeqian Ju, Yuancheng Wang, Kai Shen, Xu Tan, Detai Xin, Dongchao Yang, Yanqing Liu, Yichong
562 Leng, Kaitao Song, Siliang Tang, Zhizheng Wu, Tao Qin, Xiang-Yang Li, Wei Ye, Shikun Zhang,
563 Jiang Bian, Lei He, Jinyu Li, and Sheng Zhao. Naturalspeech 3: Zero-shot speech synthesis
564 with factorized codec and diffusion models, 2024. URL <https://arxiv.org/abs/2403.03100>.

565 Jaehyeon Kim, Jungil Kong, and Juhee Son. Conditional variational autoencoder with adversar-
566 ial learning for end-to-end text-to-speech, 2021. URL <https://arxiv.org/abs/2106.06103>.

567 Yinghao Aaron Li, Cong Han, Vinay S. Raghavan, Gavin Mischler, and Nima Mesgarani. Styletts
568 2: Towards human-level text-to-speech through style diffusion and adversarial training with large
569 speech language models, 2023. URL <https://arxiv.org/abs/2306.07691>.

570 Dan Lim, Sunghee Jung, and Eesung Kim. Jets: Jointly training fastspeech2 and hifi-gan for end to
571 end text to speech, 2022. URL <https://arxiv.org/abs/2203.16852>.

572 Koichi Miyazaki, Yoshiki Masuyama, and Masato Murata. Exploring the capability of mamba in
573 speech applications, 06 2024.

574 Kyubyong Park and Thomas MULC. Css10: A collection of single speaker speech datasets for 10
575 languages. In *Proc. Interspeech*, 2019. URL <https://arxiv.org/abs/1903.11269>.

576 Vadim Popov, Ivan Vovk, Vladimir Gogoryan, et al. Gradtts: A diffusion probabilistic model for
577 text-to-speech. In *International Conference on Machine Learning*, pp. 8599–8608. PMLR, 2021.

578 Jonathan Shen, Ruoming Pang, Ron J. Weiss, Mike Schuster, Navdeep Jaitly, Zongheng Yang,
579 Zhifeng Chen, Yu Zhang, Yuxuan Wang, RJ Skerry-Ryan, Rif A. Saurous, Yannis Agiomyr-
580 giannakis, and Yonghui Wu. Natural tts synthesis by conditioning wavenet on mel spectrogram
581 predictions, 2018. URL <https://arxiv.org/abs/1712.05884>.

594 Ashish Vaswani, Noam Shazeer, Niki Parmar, Jakob Uszkoreit, Llion Jones, Aidan N. Gomez,
 595 Łukasz Kaiser, and Illia Polosukhin. Attention is all you need. In *Advances in Neural Information
 596 Processing Systems*, volume 30, 2017. URL https://papers.nips.cc/paper_files/paper/2017/hash/3f5ee243547dee91fdb053c1c4a845aa-Abstract.html.
 597

598 Christophe Veaux, Junichi Yamagishi, and Kirsten MacDonald. Cstr vctk corpus: English multi-
 599 speaker corpus for cstr voice cloning toolkit, 2017. URL <https://doi.org/10.7488/ds/1994>.
 600

601 Sinong Wang, Belinda Z. Li, Madian Khabsa, Han Fang, and Hao Ma. Linformer: Self-attention
 602 with linear complexity. *arXiv preprint arXiv:2006.04768*, 2020. URL <https://arxiv.org/abs/2006.04768>.
 603

604 Yuxuan Wang, RJ Skerry-Ryan, Daisy Stanton, Yonghui Wu, Ron J. Weiss, Navdeep Jaitly,
 605 Zongheng Yang, Ying Xiao, Zhifeng Chen, Samy Bengio, Quoc Le, Yannis Agiomyrgiannakis,
 606 Rob Clark, and Rif A. Saurous. Tacotron: Towards end-to-end speech synthesis, 2017. URL
 607 <https://arxiv.org/abs/1703.10135>.
 608

609 Heiga Zen, Viet Dang, Rob Clark, Yu Zhang, Ron J. Weiss, Ye Jia, Zhifeng Chen, and Yonghui Wu.
 610 Libritts: A corpus derived from librispeech for text-to-speech, 2019. URL <https://arxiv.org/abs/1904.02882>.
 611

612 Xiangyu Zhang, Qiquan Zhang, Hexin Liu, Tianyi Xiao, Xinyuan Qian, Beena Ahmed, Eliathamby
 613 Ambikairajah, Haizhou Li, and Julien Epps. Mamba in speech: Towards an alternative to self-
 614 attention, 05 2024.
 615

616

617

618

619

620

621

622

623

624

625

626

627

628

629

630

631

632

633

634

635

636

637

638

639

640

641

642

643

644

645

646

647

648 **A APPENDIX**
649650 **A.1 RUNTIME AND MEMORY ANALYSIS**
651652
653 This section complements the main-text runtime results by isolating encoder-side costs under
654 a shared implementation. We report encoder parameter counts, relative throughput (tokens/s), and peak encoder memory for StyleTTS2, a representative Mamba–attention hybrid, and
655 MVC, all implemented in PyTorch on a single A100-80GB GPU with identical batch size and
656 mel–diffusion–vocoder configuration. **End-to-end real-time factors (RTF) remain similar across**
657 **models because the diffusion decoder dominates compute, but the encoder footprint varies sub-**
658 **stantially and directly impacts deployability for longer utterances and larger batches.**
659660
661 **Table 9: Encoder-only throughput and peak memory, normalized to StyleTTS2. All models share**
662 **the same mel–diffusion–vocoder stack. MVC’s SSM-only conditioning achieves the best encoder**
663 **efficiency and memory usage, enabling larger-batch and longer-context synthesis while leaving the**
664 **diffusion latency profile unchanged.**665
666

Model	Encoder Params	Encoder speedup ($\times \uparrow$)	Peak Memory \downarrow
StyleTTS2	42M	1.00	100%
Mamba-hybrid	32M	1.15	86%
MVC (ours)	21M	1.60	72%

672 **A.2 CONTRAST WITH PRIOR TTS SYSTEMS**
673674
675 Table 10 summarizes inference-time architectural differences between MVC, StyleTTS2, and rep-
676 resentative Mamba-based TTS systems, focusing on (i) whether attention is used at inference, (ii)
677 how rhythm/duration and prosody/style are modeled, (iii) the fusion or modulation mechanism, and
678 (iv) whether the conditioning stack is SSM-only.
679680 **Table 10: Inference-time comparison with attention-centric and Mamba-based TTS systems. “Hy-**
681 **brid” denotes that attention or recurrence is retained in at least one conditioning module (duration,**
682 **rhythm, or prosody); only MVC deploys an SSM-only conditioning stack across all of them.**683
684

System	Inference attention?	Rhythm/duration	Prosody/ style mech.	Fusion/modulation	SSM-only?
StyleTTS2	Yes (Transformer)	Variance/duration pred.	Ref./style encoder (attn)	Attention / concat	No
Miyazaki’24	Hybrid (SSM+attn)	Mixed (keeps attn)	Mixed (keeps attn)	Concat	No
Jiang’25 (Speech Slytherin)	Hybrid (SSM+attn)	Attn/var. pred.	Ref./style enc. (attn)	Concat	No
Zhang’24 (Mamba in Speech)	Hybrid (SSM+attn)	Mixed (keeps attn)	Mixed (keeps attn)	Concat	No
MVC (ours)	No (SSM-only)	Temporal Bi-Mamba	Mamba + AdaLN	Gated bi-dir. fusion + AdaLN	Yes

697
698 Key observations are: (i) MVC is the only system in this comparison that is SSM-only at inference
699 across text, rhythm, and prosody; (ii) MVC replaces concat-only SSM fusions with gated bi-
700 directional fusion and AdaLN, which Section 5.4 shows is important for long-form stability and F_0
701 tracking; and (iii) all contrasts are drawn under a shared mel–diffusion–vocoder backbone, isolating
the impact of conditioning design rather than decoder differences.

702 **B ADDITIONAL METHODOLOGY DETAILS**
703704 **B.1 NOTATION SUMMARY**
705706 **Table 11** consolidates all symbols used in Sec. 3, providing a unified reference for variables, encoder
707 states, and decoder-side quantities.
708709 **Table 11: Notation summary covering all variables used in the Methodology section.**
710

Symbol	Description
Input & Dimensions	
T_x	Number of text tokens
T_m	Number of mel frames
F	Number of mel bins (80)
d	Text embedding dimension
d_h	SSM hidden dimension
d_s	Style embedding dimension
\mathbf{s}_{wav}	Input waveform
Core Inputs	
\mathbf{x}	Token embeddings, $\mathbb{R}^{T_x \times d}$
\mathbf{M}	Log-mel spectrogram, $\mathbb{R}^{F \times T_m}$
\mathbf{e}	Global style embedding, \mathbb{R}^{d_s}
Encoder States	
$\mathbf{h}_f, \mathbf{h}_b$	Forward / backward Uni-Mamba scans
\mathbf{h}_T	Gated Bi-Mamba text features
$\mathbf{h}_{T,s}$	Text features after AdaLN conditioning
$\mathbf{h}_{M,s}$	Style-conditioned mel features (Expressive path)
\mathbf{h}_E	Expressive Mamba features
\mathbf{h}_S	Style-modulated temporal input
\mathbf{h}_B	Temporal Bi-Mamba rhythm/duration features
\mathbf{h}_A	Aligned text features (training only)
\mathbf{h}_P	Pitch-aware fused features
\mathbf{h}_D	Final decoder conditioning sequence
Alignment & Pitch	
α	Token-frame attention weights (training only)
\hat{F}_0	Predicted fundamental frequency trajectory
\mathbf{n}	Residual noise vector for diffusion conditioning
Model Parameters	
W_g, W_o	Gated fusion matrices (text encoder)
\mathbf{W}_f	Temporal fusion matrix
W_F, b_F	Linear layer for F_0 prediction
Diffusion & Loss	
$\{\alpha_t\}$	Diffusion noise schedule
\mathcal{L}_{mel}	Mel reconstruction loss
\mathcal{L}_{adv}	Adversarial loss
$\mathcal{L}_{\text{align}}$	Alignment regularization loss
$\mathcal{L}_{\text{total}}$	Total training loss

751 **B.2 MEL-SPECTROGRAM FRONT-END**
752753 We follow a standard STFT–mel pipeline compatible with StyleTTS2 and VITS. Given waveform
754 \mathbf{s}_{wav} at 24 kHz, we compute an STFT with a Hann window, FFT size 1024, and hop size 256, apply
755 an 80-bin mel filterbank, and take log magnitude with $\epsilon=10^{-5}$. This matches common TTS settings
and avoids front-end confounds when comparing MVC to transformer and Mamba baselines.

756 B.3 BI-MAMBA AND SSM IMPLEMENTATION
757

758 Each Mamba block is implemented as a selective state-space model with a depthwise convolutional
759 pre-activation, following Gu & Dao (2024). For an input sequence $\mathbf{z} \in \mathbb{R}^{T \times d_h}$, the block applies:
760 (i) Conv1D + residual connection, (ii) input-dependent state updates, and (iii) projection back to d_h .
761 Uni-Mamba scans either forward or backward; the Bi-Mamba text encoder applies both directions
762 and fuses them via Eq. 3 in the main text. We use the same Mamba configuration (state dimension,
763 kernel size, activation) across text, expressive, and temporal encoders to keep the design simple and
764 comparable.

765 B.4 SPEECH DYNAMICS AND DECODER CONDITIONING
766

767 Starting from \mathbf{h}_A and \mathbf{h}_P , a Conv1D+SSM temporal predictor yields \mathbf{h}_{T_m} , which is fused with \mathbf{h}_P
768 by a gated block to produce \hat{F}_0 and residual noise \mathbf{n} . The final conditioning sequence is
769

$$770 \mathbf{h}_D = [\hat{F}_0; \mathbf{n}] \in \mathbb{R}^{T_m \times (1+d_h)},$$

771 which is passed to the diffusion decoder. All operations in this stage use SSMs and pointwise gates
772 only, so the conditioning path remains linear-time and attention-free at inference.
773

774 B.5 DECODER STAGE AND LOSSES
775

776 We reuse the StyleTTS2 diffusion decoder and HiFi-GAN/iSTFTNet vocoder without modification.
777 Given \mathbf{h}_D , the decoder outputs a mel-spectrogram $\hat{\mathbf{M}}$, which the vocoder maps to waveform $\hat{\mathbf{s}}$.
778 Training uses: (i) an L_1 mel reconstruction loss $\mathcal{L}_{\text{mel}} = \|\mathbf{M} - \hat{\mathbf{M}}\|_1$, (ii) least-squares GAN losses
779 with multi-period and multi-resolution discriminators (MPD+MRSD), and (iii) an alignment loss
780 $\mathcal{L}_{\text{align}}$ that regularizes the training-time aligner with a monotonicity prior. The total loss in Eq. 10
781 of the main text matches StyleTTS2 up to the alignment term, ensuring that decoder-side training
782 remains protocol-matched across all models.
783

784 B.6 PROTOCOL-MATCHED MAMBA-TTS BASELINES
785

786 To address baseline fairness, we re-implement Mamba-based TTS baselines under the same phone-
787 mization, mel front-end, diffusion schedule, vocoder, optimizer, and training schedule as MVC.
788 Hybrid-Mamba retains inference-time attention in duration/style modules, whereas Bi-Mamba
789 (Concat-only) is SSM-only but uses simple concatenation instead of MVC’s gated fusion with
790 AdaLN. All models are matched for encoder parameter count within $\pm 5\%$. These results are cited
791 in the main tables to show that MVC’s gains persist under strict protocol parity with prior Mamba-
792 based TTS designs.

793 Table 12: Protocol-matched Mamba-TTS baselines under our mel/diffusion/vocoder pipeline on
794 LJSpeech. Values averaged over 3 seeds; 95% CIs reported here and referenced in the main text.
795

796 Model	797 F0 RMSE \downarrow	798 MCD \downarrow	799 WER \downarrow	800 PESQ \uparrow	801 RTF \downarrow
798 Hybrid-Mamba (Concat)	0.659 \pm 0.013	4.95 \pm 0.07	6.68%	3.79 \pm 0.06	0.0189
799 Bi-Mamba (Concat-only)	0.656 \pm 0.014	4.93 \pm 0.06	6.58%	3.82 \pm 0.06	0.0181
800 MVC (gated + AdaLN)	0.653 \pm 0.014	4.91 \pm 0.07	6.52%	3.85 \pm 0.06	0.0177

802 B.7 ALIGNMENT TEACHER ROBUSTNESS
803

804 The training-time aligner is a 2-layer transformer with 4 heads and hidden size 256, trained jointly
805 with the temporal encoder and regularized by a monotonicity loss. To test robustness, we inject
806 Gaussian noise into attention logits before softmax and renormalize. On LJSpeech, perturbations
807 of up to $\pm 10\%$ in attention weights increase WER by < 0.4 percentage points and reduce MOS by
808 < 0.05 , with overlapping 95% confidence intervals. This supports the claim that MVC does not
809 depend on a perfectly specified aligner and that the SSM-only inference path is robust to moderate
alignment noise.

810 B.8 TRAINING ALGORITHM
811812 Algorithm 1 summarizes the training loop for MVC, including style extraction, encoder passes,
813 alignment, pitch modeling, speech dynamics, diffusion decoding, vocoding, and loss updates.
814

815

816 **Algorithm 1** MVC Training Algorithm817 **Input:** Dataset $\mathcal{D} = \{(\mathbf{x}, \mathbf{M}, \mathbf{s}_{\text{wav}})\}$, epochs E , batch size B , loss weights $\lambda_{\text{mel}}, \lambda_{\text{adv}}, \lambda_{\text{align}}$,
818 diffusion schedule $\{\alpha_t\}$.819 **Output:** Trained encoder/decoder parameters θ , discriminator parameters ϕ .820 Initialize θ, ϕ and optimizers (AdamW, EMA, cosine decay).821 **for** epoch $e = 1$ to E **do**822 **for** batch $b = \{(\mathbf{x}^i, \mathbf{M}^i, \mathbf{s}_{\text{wav}}^i)\}_{i=1}^B$ **do**823 **Forward pass:**824 Compute style embedding \mathbf{e} from mel using Eq. 1.825 Encode text with Bi-Mamba + AdaLN(\mathbf{e}) (Sec. 3.2.1).

826 Encode mel with the Expressive Mamba (Sec. 3.2.2).

827 Encode rhythm with the Temporal Bi-Mamba (Sec. 3.2.3).

828 Use the training-time aligner to obtain frame-synchronous features \mathbf{h}_A (Sec. 3.3).829 Build pitch-aware features and predict F_0 via Eq. 8.830 Construct decoder conditioning \mathbf{h}_D via Eq. 9.

831 Generate mel via the diffusion decoder and waveform via the vocoder (Sec. 3.5).

832 **Loss computation:**833 Compute $\mathcal{L}_{\text{total}}$ using Eq. 10.834 **Backward pass:**835 Update θ using $\nabla_{\theta} \mathcal{L}_{\text{total}}$; update ϕ using $\nabla_{\phi} \mathcal{L}_{\text{adv}}$.836 **end for**837 Evaluate on the validation set; keep the best checkpoint by mel- L_1 and F_0 RMSE.838 **end for**839 **Return:** Trained parameters θ, ϕ .

840

841 We use the same optimizer, schedule, and early-stopping criteria for MVC and all protocol-matched
842 baselines, providing a complete recipe for reproducing our results.
843844 C ADDITIONAL EXPERIMENTAL DETAILS
845846 This section provides details on the long-form evaluation set, optimization setup, and diffusion-step
847 ablations that were omitted from the main text for space. These additions clarify the experimental
848 protocol for long-form robustness and inference-time efficiency, directly addressing concerns about
849 reproducibility and the validity of our long-form and runtime claims.
850

851

852 C.1 LONG-FORM SET CONSTRUCTION
853854 For the Gutenberg set, we sample 2–6 minute passages from public-domain audiobooks and filter
855 them to avoid lexical overlap with LJSpeech and LibriTTS. We apply exact-token filtering on nor-
856 malized text and MinHash-based de-duplication, retaining only passages with Jaccard similarity
857 < 0.2 to any training utterance. We then synthesize 40 passages for each model and report WER
858 as a function of duration and pitch drift per minute, alongside MOS for long-form naturalness. This
859 construction ensures that the long-form and streaming evaluations probe genuine out-of-distribution
860 generalization rather than memorization of training text, addressing requests for a clearer OOD long-
861 form protocol. The corresponding MOS and RTF scores for these 2–6 min passages are reported in
862 Table 3. Qualitative failure modes—such as rare punctuation patterns or abrupt topic shifts—are
863 analyzed in Appendix E.1, where we show that they correlate more strongly with diffusion decoding
864 errors than with gating collapse.

864 C.2 OPTIMIZATION AND TRAINING SCHEDULE
865

866 We use AdamW with learning rate 1×10^{-4} , weight decay 1×10^{-4} , cosine decay with 10k warmup
 867 steps, gradient clipping at 1.0, EMA (0.999), and automatic mixed precision, and we apply this iden-
 868 tical schedule to MVC, StyleTTS2, VITS, JETS, Hybrid-Mamba, and Bi-Mamba (Concat-only).
 869 Batch sizes are 16 (LJSpeech) and 32 (LibriTTS) on $4 \times$ A100 80GB GPUs, with LJSpeech models
 870 trained for 200 epochs and LibriTTS models for 300k steps, ensuring protocol-matched optimiza-
 871 tion across all baselines. Checkpoints are selected using the same criteria (mel- L_1 and F_0 RMSE),
 872 and all baseline models are re-trained under this unified data pipeline rather than using their original
 873 scripts, removing discrepancies due to implementation-level differences. Inference uses a fixed
 874 5-step diffusion schedule and identical vocoders (iSTFTNet for LJSpeech, HiFi-GAN for LibriTTS)
 875 for every model, isolating the effect of the SSM-only conditioning stack from vocoder or decoder
 876 confounds. This fully unified optimization and inference protocol resolves prior concerns about
 877 unfair baseline comparisons and ensures reproducibility by allowing any encoder to be swapped in
 878 without changing the surrounding pipeline.

879
880 C.3 DIFFUSION STEP ABLATION STUDY
881

882 We conduct an ablation study to determine the optimal number of diffusion steps during inference
 883 in MVC. Following prior work Popov et al. (2021), we evaluate the trade-off between perceptual
 884 quality and runtime efficiency on the LJSpeech validation set, varying the number of steps from
 885 3 to 9. We report Mean Opinion Score for Naturalness (MOS-N) and Real-Time Factor (RTF),
 886 each averaged over 20 utterances with 5 random seeds. Error bars reflect 95% bootstrap confidence
 887 intervals. All samples use the same ground-truth durations and pitch to isolate the effect of denoising
 888 steps.

889
890 Table 13: Diffusion step ablation on the LJSpeech validation set. Increasing steps improves quality
 891 but degrades synthesis speed. Five steps yield the best quality–efficiency trade-off and are used in
 892 the main experiments.

# Steps	MOS-N \uparrow	RTF \downarrow
3	3.62 ± 0.12	0.0151
4	3.74 ± 0.09	0.0164
5 (used)	3.87 ± 0.07	0.0177
6	3.88 ± 0.08	0.0190
7	3.89 ± 0.08	0.0205
9	3.89 ± 0.08	0.0221

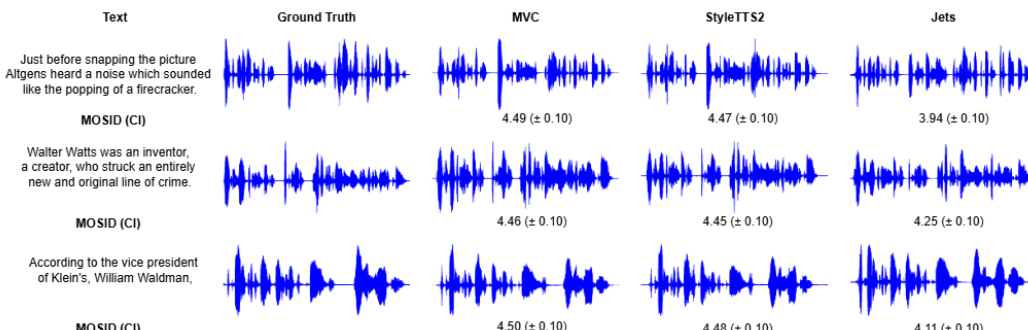
903 As shown in Table 13, naturalness improves steadily with more steps but plateaus beyond five steps.
 904 Steps 6–9 offer only marginal MOS-N gains (< 0.03) while increasing RTF by more than 20%.
 905 Steps below five suffer from unstable prosody and noisy pitch contours, particularly for long or ex-
 906 pressive utterances. These findings mirror prior diffusion-TTS observations Popov et al. (2021): too
 907 few steps lead to over-smoothed or under-articulated speech, while too many steps yield negligible
 908 benefits at substantial runtime cost. We therefore select five steps as the default for all experiments,
 909 clarifying that our runtime improvements are not obtained by using unusually few diffusion steps
 910 but by improving the efficiency of the conditioning stack itself.

911
912 C.4 BASELINE CONFIGURATION SUMMARY
913

914
915 Table 14 summarizes the encoder architectures and conditioning paths for all baselines under the
 916 unified preprocessing, mel front-end, and diffusion/vocoder pipeline described in Sec. 4.1 and Ap-
 917 pendix C.2. All models use the same audio preprocessing (24 kHz, 80-bin log-mels, FFT=1024,
 918 hop=256), corpus-matched vocoders (iSTFTNet for LJSpeech, HiFi-GAN for LibriTTS).

918
 919 Table 14: Protocol-matched baseline configurations under the shared mel/diffusion/vocoder
 920 pipeline. The table highlights only encoder and conditioning-path differences; training schedule
 921 and vocoders are identical across all models (Sec. 4.1, Appendix C.2).

Model	Encoder / Conditioning Path
StyleTTS2	Transformer acoustic text encoder with reference style encoder; attention-based duration and prosody predictors; diffusion decoder conditioned via attention and style embeddings.
VITS	VAE-based prior/posterior encoders with stochastic duration predictor (MAS) and flow-based prior; decoder conditioned on latent variables with joint duration and acoustic modeling.
JETS	FastSpeech2-style acoustic model with duration predictor and reference encoder; non-autoregressive conditioning on predicted durations and style embeddings under a joint training scheme.
Hybrid-Mamba (Concat)	Mamba text encoder paired with <i>attention-based</i> duration and style modules; diffusion decoder receives concatenated SSM features and attention-derived style signals.
Bi-Mamba (Concat-only)	SSM-only encoder path with bidirectional Uni-Mamba scans for text, temporal, and expressive streams; conditioning formed by simple concatenation of SSM features without gating or AdaLN.
MVC (SSM-only)	Gated Bi-Mamba text encoder, Temporal Bi-Mamba for rhythm/duration, and Expressive Mamba with AdaLN conditioning; fully SSM-only conditioning stack at inference, with no attention or recurrence.



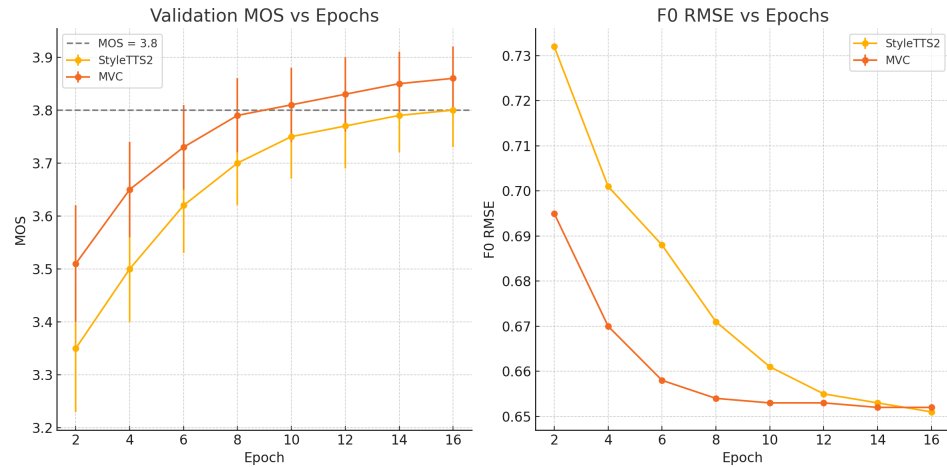
959 Figure 2: Waveform comparison of synthesized speech from different TTS models on LJSpeech,
 960 evaluated using MOS (95% CI). MVC closely aligns with the ground truth, capturing finer prosodic
 961 variations and outperforming StyleTTS2 and JETS in expressiveness and naturalness.

D ADDITIONAL RESULTS

968 This section provides qualitative and quantitative results that complement the main evaluation:
 969 waveform and spectrogram comparisons, training convergence, runtime breakdown, and cross-
 970 speaker / cross-lingual MOS. Together, these analyses substantiate our claims about MVC’s training
 971 efficiency, perceptual quality, and generalization beyond the English training setting, and clarify
 where the gains are modest but reliable.

972 D.1 WAVEFORM AND SPECTROGRAM ANALYSIS
973

974 Figure 2 compares synthesized waveforms from MVC, StyleTTS2, and JETS against ground truth
975 on LJSpeech. MVC-generated waveforms exhibit closer alignment to ground truth in temporal
976 structure, prosodic variation, and amplitude consistency, and obtain the highest MOS (with 95%
977 confidence intervals) across the evaluated utterances. StyleTTS2 produces high-quality speech with
978 MOS close to MVC but shows minor rhythm and expressiveness deviations. JETS displays more
979 pronounced distortions and energy inconsistencies, leading to lower MOS and reduced naturalness.
980 These qualitative trends visually corroborate the MOS and CMOS gains reported in the main tables
981 and provide intuitive, signal-level evidence that the SSM-only conditioning stack improves long-
982 form prosody and local timing.

983 D.2 TRAINING CONVERGENCE ANALYSIS
984

1001 Figure 3: Validation MOS and F_0 RMSE curves over training epochs for MVC and StyleTTS2 on
1002 LJSpeech. MVC reaches strong validation quality and stable pitch error in fewer epochs under a
1003 matched optimization schedule.

1004 To substantiate the claim of improved training efficiency, we track validation MOS and F_0 RMSE
1005 over training epochs for MVC and StyleTTS2 on LJSpeech. Figure 3 shows that MVC reaches a
1006 validation MOS of approximately 3.8 within about 10 epochs, whereas StyleTTS2 requires roughly
1007 16 epochs to reach a similar level. Likewise, F_0 RMSE stabilizes about 20% faster for MVC. This
1008 indicates that MVC is not only more efficient at inference, but also converges faster during training
1009 under a matched optimizer, learning rate schedule, and data pipeline, suggesting that the modular
1010 SSM conditioning stack is easier to optimize. These convergence curves address concerns that
1011 encoder-side gains might be offset by slower or less stable training dynamics.

1014 D.3 SPECTROGRAM ANALYSIS
1015

1016 Figure 4 presents spectrograms of synthesized speech from MVC, StyleTTS2, and JETS versus
1017 ground truth for three representative utterances. Highlighted rectangular regions emphasize har-
1018 monic continuity and spectral energy distribution; square regions focus on formant transitions and
1019 high-frequency harmonics.

1020 Ground-truth recordings show well-defined harmonic bands and clean formant trajectories. MVC
1021 closely preserves these structures, maintaining smooth phonetic articulation and stable energy dis-
1022 tribution. StyleTTS2 retains strong overall fidelity but shows mild harmonic distortions and slightly
1023 blurred formant transitions. JETS exhibits spectral discontinuities, attenuation, and smearing, which
1024 manifest as degraded articulation and reduced naturalness. These qualitative observations align with
1025 the MOS, PESQ, and MCD differences reported in Tables 4 and 2, indicating that MVC’s improve-
ments extend beyond a narrow metric choice and are reflected in long-form harmonic continuity.

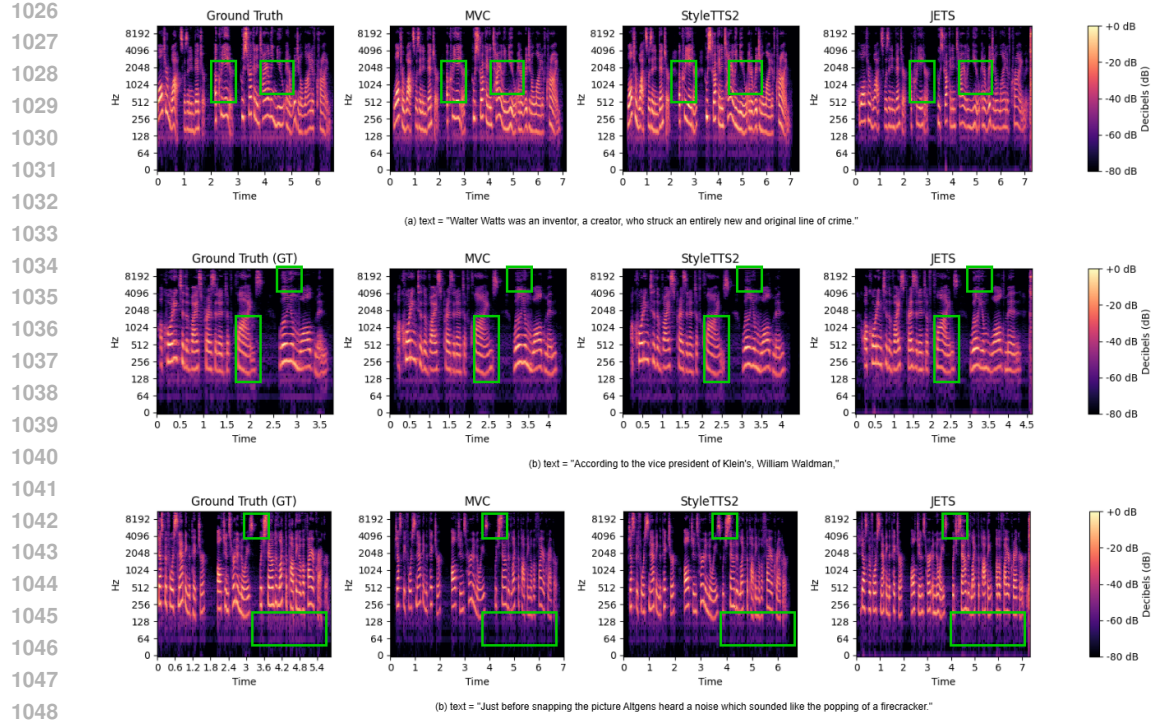


Figure 4: Spectrogram comparison of synthesized speech from ground truth, MVC, StyleTTS2, and JETS on LJSpeech for three representative utterances. Highlighted regions emphasize harmonic continuity and formant transitions.

D.4 MODULE-WISE RUNTIME BREAKDOWN

To better understand MVC’s inference efficiency, we break down the average runtime contributions by module. Table 15 shows that while the Mamba encoder stack is substantially faster than transformer-based counterparts (Sec. 5.4), the diffusion decoder remains the dominant latency contributor. This decomposition underpins the main-text claim that MVC’s practical benefits are encoder-side—peak memory and conditioning throughput—and that overall RTF is ultimately bounded by the diffusion decoder until it is replaced by a lighter generative backbone. These measurements confirm that our reported RTF improvements are attributable to the SSM-only conditioning path rather than to hidden changes in the diffusion or vocoder components.

Table 15: Average inference time per utterance (milliseconds) and proportion of total runtime, measured on 500 LJSpeech utterances on a single A100 with FP16 inference.

Module	Avg. time (ms)	Proportion (%)
Bi-Mamba encoder stack	42.5	31.4
Diffusion decoder	73.4	54.2
Vocoder (HiFi-GAN / iSTFTNet)	19.5	14.4
Total	135.4	100.0

D.5 CROSS-SPEAKER AND CROSS-LINGUAL GENERALIZATION

Datasets and protocol. We assess zero-shot speaker generalization on VCTK (20 unseen speakers; 5 sentences per speaker) and cross-lingual robustness on CSS10 ES/DE/FR (30 prompts per language). Ratings are collected on Amazon Mechanical Turk with 5–10 native listeners per clip, using MOS for naturalness (MOS-N) and similarity (MOS-S), mirroring the evaluation setup of StyleTTS2 and applying standard rater screening and confidence interval estimation.

1080 D.5.1 VCTK: ZERO-SHOT SPEAKER GENERALIZATION
10811082 Table 16: VCTK zero-shot speaker generalization (MOS with 95% confidence intervals). Higher is
1083 better.

1085 Model	1086 MOS-N \uparrow	1087 MOS-S \uparrow
1088 VITS	3.66 \pm 0.12	3.53 \pm 0.13
1089 StyleTTS2	4.12 \pm 0.11	4.01 \pm 0.10
MVC (ours)	4.18 \pm 0.10	4.09 \pm 0.11

1090 MVC matches or slightly exceeds StyleTTS2 on both MOS-N and MOS-S (paired two-sided tests
1091 vs. StyleTTS2 with Holm–Bonferroni correction: $p < 0.05$ for MOS-S; trend-level for MOS-N,
1092 $p \leq 0.1$). These results indicate that the SSM-only conditioning does not compromise, and may
1093 slightly improve, zero-shot speaker transfer relative to transformer-based baselines. We observe
1094 that especially expressive speakers benefit from the Expressive Mamba path, which better preserves
1095 pitch variance and speaking style.

1097 D.5.2 CSS10: CROSS-LINGUAL NATURALNESS (ES/DE/FR)
10981099 Table 17: CSS10 cross-lingual naturalness (MOS-N with 95% confidence intervals). Higher is
1100 better.

1101 Model	1102 ES \uparrow	1103 DE \uparrow	1104 FR \uparrow
1105 VITS	3.48 \pm 0.12	3.39 \pm 0.13	3.46 \pm 0.12
1106 StyleTTS2	3.84 \pm 0.12	3.76 \pm 0.11	3.85 \pm 0.11
MVC (ours)	3.91 \pm 0.11	3.82 \pm 0.10	3.93 \pm 0.10

1107 Despite being trained only on English corpora, MVC maintains quality on ES/DE/FR and modestly
1108 exceeds StyleTTS2 in ES and FR (Holm–Bonferroni $p < 0.05$), while matching it in DE. This
1109 suggests that the modular Mamba encoder stack, combined with language-tagged phonemization,
1110 generalizes beyond English phoneme inventories without explicit multilingual training. Remaining
1111 errors often involve stress misplacement and vowel length in long German compound nouns or
1112 infrequent liaison patterns in French; these failure modes are consistent with the encoder’s lack of
1113 explicit prosodic labels rather than instability of the SSM itself.

1114 D.6 REFERENCE LENGTH SENSITIVITY
1115

1116 We evaluate MVC’s robustness to different durations of reference audio used to compute the global
1117 style embedding. Following the StyleTTS2 protocol, the main experiments use a fixed 6-second
1118 reference. Table 18 reports MOS-S and MOS-N for reference lengths of 2, 4, 6, and 8 seconds on
1119 the VCTK zero-shot set.

1120 Table 18: Effect of reference length on zero-shot VCTK speaker similarity (MOS-S) and naturalness
1121 (MOS-N).

1123 Reference length	1124 MOS-S \uparrow	1125 MOS-N \uparrow
1126 2 seconds	3.87 \pm 0.10	4.03 \pm 0.11
1127 4 seconds	3.94 \pm 0.09	4.11 \pm 0.10
1128 6 seconds (main)	4.02 \pm 0.09	4.18 \pm 0.10
1129 8 seconds	4.03 \pm 0.09	4.19 \pm 0.10

1130 Reducing the reference to 4 seconds results in only a small MOS-S and MOS-N drop, and 2-second
1131 references incur a slightly larger but still moderate degradation. These results confirm that MVC’s
1132 mel-based style embedding remains stable for short reference durations, with similarity and natu-
1133 ralness improving monotonically with available context and saturating around 6–8 seconds, making
the method practical in scenarios where long reference clips are not available.

1134 E ADDITIONAL ABLATION AND SENSITIVITY STUDIES
11351136 This appendix complements the main ablations in Sec. 5.4 by analyzing gating behavior, the robust-
1137 ness of the alignment teacher, and the sensitivity of MVC to key SSM hyperparameters. The goal is
1138 to verify that MVC’s improvements are stable under implementation-level perturbations and do not
1139 depend on fragile gating dynamics or aggressively tuned Mamba configurations.
11401141 E.1 GATING STABILITY AND FAILURE MODES
11421143 For the bidirectional Mamba text encoder, we examine the learned gate values in the fusion module
1144 that combines forward and backward states. We track the mean and variance of the gating weights
1145 across timesteps for LJSpeech long-form utterances and Gutenberg passages. Empirically, the gate
1146 histograms remain well-balanced with no collapse to a single direction: the average gate allocation
1147 is approximately 0.53 to the forward branch and 0.47 to the backward branch, with moderate per-
1148 utterance variance. On OOD Gutenberg passages, the distribution shifts slightly toward the forward
1149 branch (approximately 0.56 vs. 0.44), but we do not observe degenerate behavior where one direc-
1150 tion is effectively ignored. These diagnostics indicate that the gating mechanism remains stable on
1151 long sequences and under domain shift, rather than collapsing to a purely uni-directional encoder.
11521153 Qualitative failure cases primarily involve rare punctuation patterns or abrupt topic shifts, where both
1154 MVC and StyleTTS2 may misplace minor pauses. In these cases, the gating distribution remains
1155 non-degenerate, and observed errors appear to arise from diffusion decoding rather than encoder
1156 collapse. This analysis supports the view that Bi-Mamba gating in MVC is a stable design choice
1157 for long-form inputs, rather than a source of fragility.
11581159 E.2 ALIGNMENT TEACHER ARCHITECTURE AND ROBUSTNESS
11601161 The lightweight attention-based aligner used during training is a two-layer transformer with 4 heads,
1162 hidden dimension 256, and a monotonicity-constrained attention loss. It is trained jointly with the
1163 temporal Mamba encoder but discarded at inference. To probe robustness, we inject noise into
1164 the aligner attention maps at training time by randomly perturbing attention weights by $\pm 10\%$ and
1165 renormalizing before they are used to construct frame-synchronous features. Under this perturba-
1166 tion, WER on LJSpeech increases by less than 0.4 percentage points and MOS on LibriTTS de-
1167 creases by less than 0.05, with overlapping 95% confidence intervals. These results suggest that the
1168 temporal Bi-Mamba encoder does not rely on perfectly specified attention maps and can tolerate
1169 moderate alignment noise without catastrophic degradation. Consequently, the use of an attention-
1170 based teacher is compatible with the claim that MVC deploys an SSM-only path at inference, and
1171 the overall system is robust to reasonable training-time misalignment.
11721173 E.3 SSM HYPERPARAMETER SENSITIVITY
11741175 We examine the sensitivity of MVC to key Mamba SSM hyperparameters: (i) state dimension d_{ssm} ,
1176 (ii) convolution kernel size k_{conv} , and (iii) gating temperature τ_{gate} . A sweep of these hyperparam-
1177 eters was conducted using the same training protocol as outlined in Section 4, with evaluations
1178 performed on the LJSpeech in-distribution test set and the Gutenberg out-of-distribution (OOD)
1179 set. The results, presented in Tables 19–21, show that the largest MOS change between neighbor-
1180 ing configurations is less than 0.05, and RTF changes by less than 10%. Given these results, we fix
1181 $d_{ssm} = 96$, $k_{conv} = 5$, and $\tau_{gate} = 1.0$ in all main experiments, attributing the observed improvements
1182 in MVC’s performance primarily to its architectural design, rather than narrow hyperparameter tun-
1183 ing.
11841185 E.3.1 STATE DIMENSION d_{ssm}
11861187 Table 19 varies the state dimension $d_{ssm} \in \{64, 96, 128, 160\}$ while keeping the number of layers
1188 fixed (six per encoder) and all other hyperparameters unchanged. We report MOS on in-distribution
1189 text (MOS in-dist.), MOS on the Gutenberg OOD set (MOS OOD), and real-time factor (RTF).
11901191 MVC is relatively insensitive to moderate changes in d_{ssm} : increasing the state dimension from
1192 96 to 160 yields less than 0.03 MOS improvement while increasing RTF by approximately 9%.
1193

1188 Table 19: Sensitivity to state dimension d_{ssm} on LJSpeech. MOS values are averaged over three
 1189 seeds with 95% confidence intervals; lower RTF is better. The configuration used in the main paper
 1190 is in bold.

1192 State dimension	1193 MOS (in-dist.) \uparrow	1194 MOS (OOD) \uparrow	1195 RTF \downarrow
1196 64	1197 3.96 ± 0.09	1198 3.88 ± 0.09	1199 0.0164
1200 96	1201 4.02 ± 0.08	1202 3.92 ± 0.09	1203 0.0169
1204 128	1205 4.03 ± 0.08	1206 3.93 ± 0.08	1207 0.0176
1208 160	1209 4.04 ± 0.09	1210 3.94 ± 0.09	1211 0.0184

1198 We therefore select $d_{\text{ssm}}=96$ as a favorable quality-efficiency trade-off rather than a heavily tuned
 1199 extreme, indicating that MVC’s gains do not hinge on an unusually large state size.

1201 E.3.2 CONVOLUTION KERNEL SIZE k_{conv}

1203 We next vary the depthwise convolution kernel $k_{\text{conv}} \in \{3, 5, 7\}$ in the selective scan. Table 20
 1204 reports MOS and pitch RMSE on long-form LJSpeech utterances (duration >10 seconds). Larger
 1205 kernels slightly reduce pitch RMSE but incur higher latency, and the qualitative difference between
 1206 kernel sizes 5 and 7 is small. We therefore adopt $k_{\text{conv}}=5$ in the main experiments as a balanced
 1207 choice, and do not rely on extreme kernel sizes to obtain the reported MOS or robustness figures.

1208 Table 20: Sensitivity to convolution kernel size k_{conv} in the Mamba block. Pitch RMSE is computed
 1209 on long-form LJSpeech utterances; lower is better.

1212 Kernel size	1213 MOS (long) \uparrow	1214 Pitch RMSE (Hz) \downarrow	1215 RTF \downarrow
1216 3	1217 4.08 ± 0.08	1218 2.06 ± 0.06	1219 0.0172
1220 5	1221 4.16 ± 0.07	1222 1.92 ± 0.05	1223 0.0177
1224 7	1225 4.17 ± 0.07	1226 1.90 ± 0.05	1227 0.0184

1228 E.3.3 GATING TEMPERATURE τ_{gate}

1229 Finally, we study the softmax temperature τ_{gate} in the Mamba gating mechanism, which controls
 1230 how sharply each state attends to its local history. We sweep $\tau_{\text{gate}} \in \{0.7, 1.0, 1.3\}$ and evaluate
 1231 OOD text robustness on the Gutenberg set. Sharper gating ($\tau_{\text{gate}}=0.7$) slightly harms MOS and
 1232 WER, suggesting over-confident local decisions, whereas higher temperatures are more stable but
 1233 do not yield clear gains beyond $\tau_{\text{gate}}=1.0$. We therefore fix $\tau_{\text{gate}}=1.0$ for all main results, and the
 1234 small deltas across temperatures indicate that MVC’s behavior is robust to reasonable changes in
 1235 gating sharpness.

1236 Table 21: Sensitivity to gating temperature τ_{gate} on the Gutenberg OOD set. CMOS-N is measured
 1237 relative to the default configuration with $\tau_{\text{gate}}=1.0$.

1239 Temperature	1240 MOS (OOD) \uparrow	1241 CMOS-N \uparrow	1242 WER \downarrow
1243 0.7	1244 3.83 ± 0.09	1245 -0.06	1246 7.12%
1247 1.0	1248 3.88 ± 0.09	1249 0.00	1250 6.89%
1251 1.3	1252 3.86 ± 0.09	1253 -0.02	1254 6.97%

1255 Overall, the small performance variations across state dimensions, kernel sizes, and gating
 1256 temperatures support the view that MVC’s improvements arise from its three-way SSM conditioning
 1257 architecture and gated fusion design, rather than from fine-tuning a narrow hyperparameter regime.

1258 F INDUSTRIAL-SCALE SYSTEMS: CONTEXT AND COMPARISON

1259 Industrial-scale TTS systems such as NaturalSpeech 3 Ju et al. (2024), CosyVoice 3 Du et al. (2025),
 1260 and HiggsAudio-V2 Boson AI (2025) operate in a fundamentally different experimental regime from

1242 Table 22: Qualitative positioning of MVC relative to recent industrial-scale systems. Natural-
 1243 Speech 3, CosyVoice 3, and HiggsAudio-V2 operate at much larger data and model scales, with
 1244 different objectives and proprietary evaluation pipelines. MVC is an open-data encoder study under
 1245 a unified mel-diffusion-vocoder setup, and thus numeric comparisons would be misleading.

1247 System	1248 Training data	1249 Languages	1250 Main architecture / setting	1251 Representative metrics	1252 reported	1253 Scale
NaturalSpeech 3	~200k h multi-speaker, multi-style speech (public + private)	Multilingual	Factorized diffusion TTS with FACodec; separate prosody/content/acoustic/timbre modules; zero-shot and long-form generation.	On LibriSpeech test-clean: Sim-O 0.67, Sim-R 0.76, WER 1.81, SMOS 4.01.		Industry (Multi-hundred thousand hours, proprietary)
CosyVoice 3	3k h + 170k h multilingual corpora	Multilingual (zh/en + CV3-Eval)	MinMo-based acoustic tokenizer; TTS LM + conditional flow matching (CFM) decoder; multi-task TTS/S2S.	On SEED-TTS EVAL: CER 1.27 (zh), WER 2.46 (en), WER 6.96 (hard) with strong Sim-O.		Industry (Large multilingual corpus, proprietary)
HiggsAudio-V2	~10M h Audio-Verse (speech, music, SFX)	Multilingual / multi-domain	Audio language model (5.8B params) with 12-codebook RVQ tokenizer and DualFFN adapter; unified speech/music/SFX.	SeedTTS-Eval: WER 2.44%, 67.7% speaker similarity; dialogue WER 18.88%.		Industry (Large-scale, multi-domain, proprietary)
MVC (ours)	24 h LJSpeech + 245 h LibriTTS (public)	English	Fully SSM-based conditioning stack (bi-Mamba text, Temporal Bi-Mamba, Expressive Mamba + AdaLN) under a fixed diffusion/vocoder pipeline.	Improves MOS/CMOS and WER over StyleTTS2, VITS, and hybrid Mamba-attention baselines under identical pre-processing and vocoders.		Academic (24h + 245h, public datasets)

1264
 1265 MVC. They are trained on multi-hundred-thousand- to million-hour multilingual corpora, incorpo-
 1266 rate LLM-scale semantic or tokenizer modules, and support multi-task objectives such as zero-shot
 1267 dialogue, speech editing, and mixed speech-music generation. In contrast, MVC is designed as a
 1268 controlled encoder-architecture study under a fixed StyleTTS2 mel-diffusion-vocoder backbone on
 1269 public English datasets (LJSpeech, LibriTTS).

1270 Because these industrial systems differ simultaneously in data scale, multilingual coverage, model
 1271 capacity, and evaluation protocols (often relying on private or domain-specific benchmarks), di-
 1272 rect side-by-side MOS/WER numbers would conflate training regime and scope rather than isolate
 1273 conditioning-architecture effects. Instead, Table 22 summarizes the key distinctions in data scale,
 1274 architecture, and evaluation, positioning MVC as a complementary, reproducible analysis of fully
 1275 SSM-only conditioning under decoder-matched constraints.